

Generation of CD19-chimeric antigen receptor modified CD8⁺ T cells derived from virus-specific central memory T cells

*Seitaro Terakura,¹ *Tori N. Yamamoto,¹ Rebecca A. Gardner,¹ Cameron J. Turtle,^{1,2} Michael C. Jensen,^{1,3,4} and Stanley R. Riddell^{1,2,5}

¹Program in Immunology, Fred Hutchinson Cancer Research Center, Seattle, WA; ²Department of Medicine, University of Washington, Seattle, WA; ³Center for Childhood Cancer Research, Seattle Children's Research Institute, Seattle, WA; ⁴Department of Pediatrics, University of Washington, Seattle, WA; and ⁵Institute of Advanced Study, Technical University of Munich, Munich, Germany

The adoptive transfer of donor T cells that have been genetically modified to recognize leukemia could prevent or treat leukemia relapse after allogeneic HSCT (allo-HSCT). However, adoptive therapy after allo-HSCT should be performed with T cells that have a defined endogenous TCR specificity to avoid GVHD. Ideally, T cells selected for genetic modification would also have the capacity to persist in vivo to ensure leukemia eradication. Here, we provide a strategy for deriving virus-specific

T cells from CD45RA⁻CD62L⁺CD8⁺ central memory T (T_{CM}) cells purified from donor blood with clinical grade reagents, and redirect their specificity to the B-cell lineage marker CD19 through lentiviral transfer of a gene encoding a CD19-chimeric Ag receptor (CAR). Virus-specific T_{CM} were selectively transduced by exposure to the CD19 CAR lentivirus after peptide stimulation, and bi-specific cells were subsequently enriched to high purity using MHC streptamers. Activation of bi-specific

T cells through the CAR or the virus-specific TCR elicited phosphorylation of downstream signaling molecules with similar kinetics, and induced comparable cytokine secretion, proliferation, and lytic activity. These studies identify a strategy for tumor-specific therapy with CAR-modified T cells after allo-HSCT, and for comparative studies of CAR and TCR signaling. (*Blood*. 2012; 119(1):72-82)

Introduction

Allogeneic HSCT (allo-HSCT) is the most effective postconsolidation therapy for high-risk B-cell acute lymphocytic leukemia (B-ALL) in adults and can cure a fraction of pediatric and adult patients with ALL who relapse after conventional chemotherapy.¹⁻⁴ However, leukemia relapse remains a common cause of failure after allo-HSCT, and treatment of ALL that has recurred after transplant, either with additional chemotherapy or with donor lymphocyte infusions to enhance a GVL effect is mostly unsuccessful and can cause GVHD.¹⁻⁷ Thus, after transplantation therapies that augment the GVL effect without GVHD are needed to improve the survival of B-ALL patients, and could benefit other patients with aggressive B-cell malignancies that undergo allo-HSCT.⁸ Adoptive T-cell immunotherapy is an attractive approach to augment the GVL effect to reduce relapse, but in the context of allo-HSCT this requires that the infused T cells specifically target leukemia cells, lack alloreactivity to avoid GVHD, and have the capacity to persist in vivo sufficiently long to eradicate all malignant cells.⁹⁻¹¹

Chimeric Ag receptors (CARs) typically consist of a single-chain variable fragment (scFv) derived from a mAb specific for a tumor cell-surface molecule linked to one or more T-cell signaling moieties to activate effector function.^{12,13} CAR-modified T cells can be rapidly generated by gene transfer and are MHC independent, which circumvents the need to isolate HLA-restricted tumor-specific T cells. Most B-cell malignancies including B-ALL typically express cell-surface CD19 and several groups have developed CD19-specific CARs that are

being tested in clinical trials in patients with advanced B-cell malignancies, with anecdotal reports of therapeutic activity.¹⁴⁻¹⁶ The use of CAR-modified T cells could also provide a GVL effect after allo-HSCT, but it would be desirable to engineer donor T cells that have a predefined TCR specificity to avoid GVHD. The approach we have taken is to modify (CMV- and EBV-specific CD8⁺ T cells because large numbers of donor virus-specific T cells have previously been administered to allo-HSCT recipients without causing GVHD.¹⁷⁻¹⁹ A second issue in adoptive immunotherapy is that effector T (T_E) cells that have been expanded in vitro often persist poorly in vivo, and fail to exhibit a sustained antitumor effect.^{11,15,20} Our laboratory has previously identified a role for cell intrinsic properties of distinct memory T-cell subsets in determining cell fate after adoptive transfer and shown that T_E cells derived from central memory T (T_{CM}) cells not from effector memory T (T_{EM}) cells are capable of persisting long-term.²¹⁻²³ Here, we describe the development of clinical selection methods for purifying T_{CM} from peripheral blood and deriving and genetically modifying CMV- and EBV-specific T_E to express a CD19-specific CARs from the T_{CM} subset. Functional analysis of signaling through the CD19-CARs and the endogenous TCR on T_{CM}-derived bi-specific T_E cells demonstrated nearly equivalent activation of intracellular signaling pathways and activation of effector functions, including T-cell proliferation. These findings provide a strategy for performing adoptive T-cell therapy after allo-HSCT to augment the GVL effect with T cells of defined specificity and subset derivation.

Submitted July 13, 2011; accepted October 8, 2011. Prepublished online as *Blood* First Edition paper, October 26, 2011; DOI 10.1182/blood-2011-07-366419.

*S.T. and T.N.Y. contributed equally.

The online version of this article contains a data supplement.

The publication costs of this article were defrayed in part by page charge payment. Therefore, and solely to indicate this fact, this article is hereby marked "advertisement" in accordance with 18 USC section 1734.

© 2012 by The American Society of Hematology

Methods

Cell lines

Raji and K562 cell lines were obtained from the ATCC, Jeko-1 and BALL-1 were provided by Dr Oliver Press (Fred Hutchinson Cancer Research Center). TM-LCL is a CD19⁺ EBV-transformed lymphoblastoid cell line (LCL) that has been optimized for use as a feeder cell for T-cell culture. Cell lines were cultured in RPMI-1640 medium containing 10% FBS, 0.8mM L-glutamine, and 1% penicillin-streptomycin.

K562 cells were transduced with retroviruses that encode CD80 and CD86, and selected to > 90% purity by cell sorting for expression of these costimulatory ligands. CD80 and CD86⁺ K562 cells were then transduced with retroviruses that encode either a truncated cell-surface CD19 molecule or full-length HLA-A*0201 or B*0702 (Phoenix-Ampho system; Orbigen), and sorted twice to obtain cells of > 95% purity that expressed CD19 or HLA class I, respectively (supplemental Figure 1, available on the *Blood* Web site; see the Supplemental Materials link at the top of the online article). The truncated CD19 construct consisted of the entire extracellular and transmembrane domains and only 4 aa of the cytoplasmic tail to abrogate signaling after ligation.²¹ Cell sorting was performed on a FACSAria (BD Biosciences). For preparation of peptide-pulsed K562/HLA, the cells were washed once, resuspended in AIM-V medium (Invitrogen), and pulsed with the corresponding synthetic peptide at 5 μg/mL at room temperature for 2 hours. The cells were then washed once, irradiated (80 Gy), and used in stimulation assays.

Peptides

The following peptides were synthesized (GenScript) and provided at > 90% purity: VTEHDTLLY (HLA-A*0101_{CMVpp50}), NLVPMVATV (HLA-A*0201_{CMVpp65}), TPRVTGGGAML (HLA-B*0702_{CMVpp65}), GLCTLVAML (HLA-A*0201_{EBV-BMLF1}), and RAKFKQLL (HLA-B*0801_{EBV-BZLF1}). The peptides were dissolved in DMSO and stored at -20°C.

Separation of CD45RA⁻CD8⁺CD62L⁺ central memory T cells

Blood samples were obtained from healthy donors under protocols approved by the Fred Hutchinson Cancer Research Center Institutional Review Board. PBMCs were isolated by centrifugation of whole blood using Histopaque-1077 (Sigma-Aldrich). A CD45RA⁻CD8⁺ cell fraction was enriched by depletion of CD4⁺, CD14⁺ and CD45RA⁺ cells on the AutoMACS or CliniMACS device using clinical grade mAbs conjugated to paramagnetic beads (Miltenyi Biotec). The CD62L⁺ cells were then enriched from the depleted fraction by positive selection with a clinical grade biotin-conjugated anti-CD62L mAb (DREG56 clone; City of Hope Cancer Research Center) and anti-biotin microbeads (Miltenyi Biotec).

Lentivirus vector construction

The composition of the CD19CAR-CD28 transgene was described previously.¹⁴ The construct was modified to contain a transduction and selection marker downstream of a T2A sequence that consisted of a truncated version of the epidermal growth factor receptor (tEGFR) that lacks the EGF binding and intracellular signaling domains.^{24,25} Cell-surface tEGFR can be detected by biotinylated anti-EGFR (Erbtux) mAb.

Generation, expansion, and selection of CD19-CAR-transduced virus-specific CTLs

The enriched CD8⁺CD62L⁺ T cells were plated either in 96-well round-bottom plates at 10⁴ cells/well with 10⁴ autologous γ-irradiated (35 Gy), peptide-pulsed PBMCs, or at 10⁶ cells/well with 10⁶ autologous γ-irradiated (35 Gy) peptide-pulsed PBMCs in 24-well plates in RPMI 1640 with 10% human serum (culture medium [CM]) and 50 IU/mL IL-2. In some experiments, monocyte-derived dendritic cells

(DCs) prepared as described²⁶ were pulsed with peptide and used as an APC. Peptide-pulsed PBMCs and DCs were prepared by suspending the cells in AIM-V medium with the respective synthetic peptide at 5 μg/mL for 2 hours at 37°C. On day 1 after stimulation, the T cells were exposed to lentivirus supernatant encoding the CD19-CAR at a multiplicity of infection of 3 in the presence of polybrene at 2 μg/mL (Chemicon International) followed by spinfection (32°C, 500g, 45 minutes). On day 2, the CM was changed, and after 8-10 days of culture the cells were pooled and analyzed by flow cytometry after staining with virus-specific HLA tetramers, and with anti-EGFR and anti-Fc Abs.

The transduced T cells were expanded in culture by plating with γ-irradiated TM-LCL at various responder to stimulator ratios in CM, and fed with IL-2 50 IU/mL on days 1, 4, and 7. After 10-14 days of culture, cells were counted and stained with virus-specific HLA tetramers and Abs specific for transduction markers. The virus-specific subset of transduced T cells was then purified using reversible class I MHC streptamers as described.²⁷ D-biotin was added to dissociate the class I MHC streptamer from the T cells after selection.

Flow cytometry

All samples were analyzed by flow cytometry on Canto II or Calibur (BD Biosciences) instruments and the data were analyzed using FlowJo software (TreeStar). The starting PBMCs and each of the separated fractions were analyzed for CD4, CD14, CD8, CD45RA, and CD62L to determine selection purity and yield, and the final product was analyzed for CD13, CD16, CD19, and CD56 to identify the phenotype of contaminating cells. Cells were further classified by staining with CD62L, CD45RA, CD27, CD28, and CD127 mAbs (BD Biosciences) before and after culture. PE-conjugated HLA class I tetramers folded with CMV or EBV peptides were used to stain virus-specific TCRs (Beckman Coulter). Biotinylated ErbTux and streptavidin-PE were used to identify T cells that expressed tEGFR, and surface expression of the CD19-CAR was confirmed by staining with a FITC-conjugated goat anti-human Fcγ (Jackson ImmunoResearch Laboratories).

Intracellular cytokine staining

Bi-specific T_E cells were activated with either untransduced, CD19-transduced, or class I HLA-transduced and peptide-pulsed K562 cells in the presence of brefeldin A (Sigma-Aldrich), and then fixed and permeabilized with the Fix and Perm kit (BD Biosciences). After fixation, the T cells were stained with anti-IFN-γ, TNF-α, and IL-2 mAbs (BD Biosciences). Before fixation, anti-CD8 or tetramer staining was used to analyze surface coexpression of CD8 or virus-specific TCR, respectively. As a positive control for cytokine production, cells were stimulated with 10 ng/mL phorbol myristate acetate (PMA) and 500 ng/mL ionomycin (Sigma-Aldrich).

Intracellular phospho-flow analysis

Bi-specific T_E cells and K562 cells that expressed CD19 or viral peptide/HLA complexes were mixed at a 1:5 ratio, spun down briefly, and incubated for various times at 37°C. Cells were then fixed by the addition of 2% paraformaldehyde at 37°C for 10 minutes, permeabilized in ice-cold 90% methanol, and left on ice for 30 minutes. For staining, the following phospho-specific Abs were used: CD3ζ (pY142), ZAP70 (pY292), ZAP70 (pY319)/Syk (pY352), and p38 MAPK (pT180/pY182; all PE-conjugated; BD Biosciences); Erk1/2 (pT202/pY204; ERK), and SAPK/JNK (pT183/pY185; JNK; unconjugated; Cell Signaling Technology); bovine anti-rabbit IgG-FITC (secondary Ab; Santa Cruz Biotechnology).

Cytotoxicity assay and cytokine multiplexed bead assay

Target cells were labeled for 2 hours with ⁵¹Cr, washed twice, dispensed at 2 × 10³ cells/well into triplicate cultures in 96-well, round-bottom plates, and incubated for 4 hours at 37°C with CM at various E:T ratios. Percent-specific lysis was calculated using the standard formula.²⁸

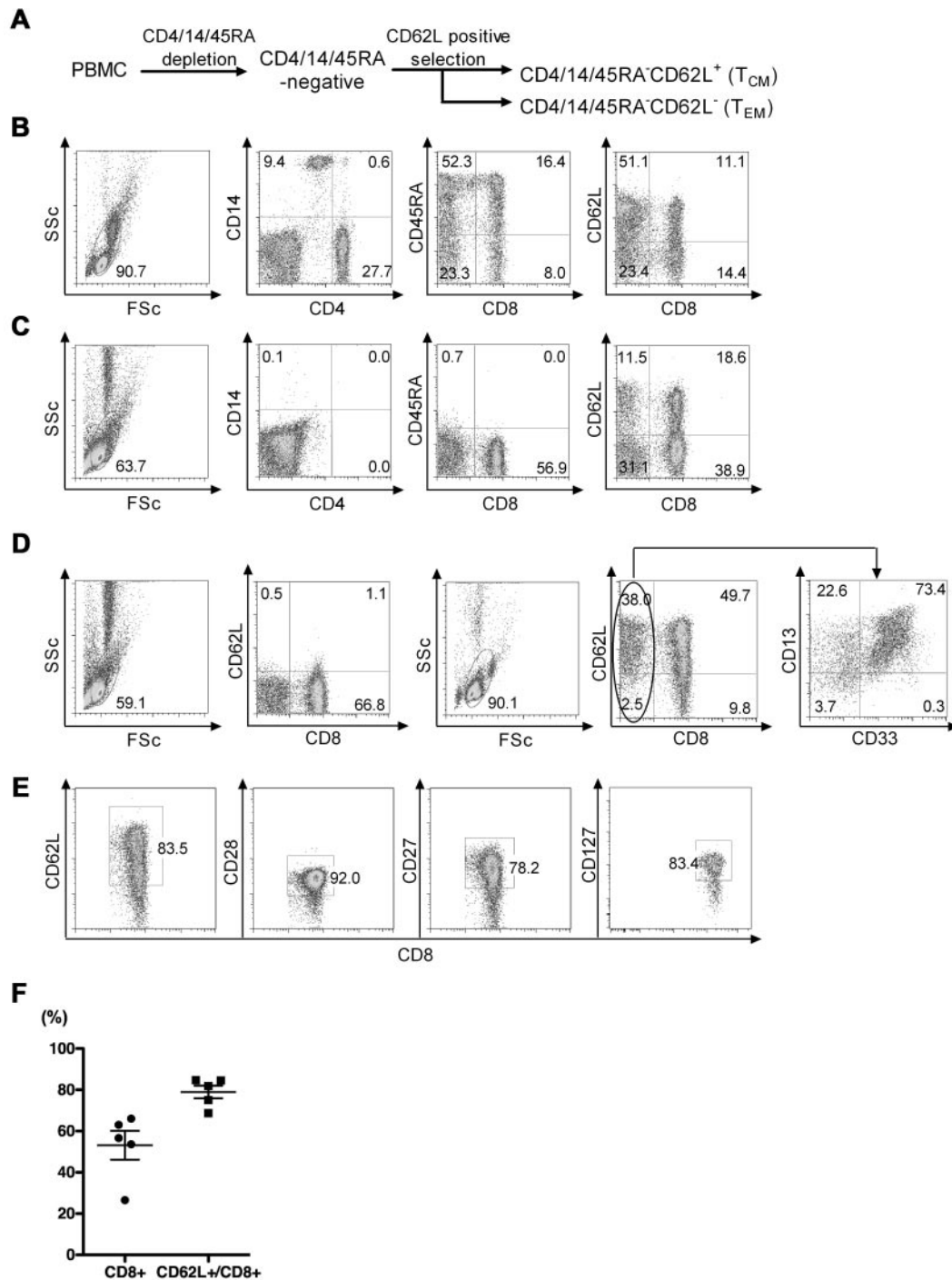


Figure 1. Enrichment of CD8⁺ T_{CM} from PBMCs with clinical grade reagents. (A) Schematic of 2-step immunomagnetic bead enrichment of CD8⁺ T_{CM}. CD4⁺/14⁺/45RA⁺ cells were removed from PBMCs by negative selection with directly conjugated immunomagnetic beads and CD62L⁺ cells were then positively selected from the remaining population with a biotinylated anti-CD62L mAb and anti-biotin beads. (B) Representative flow plots of PBMC before selection showing the frequencies of CD4⁺, CD14⁺, CD45RA⁺, CD8⁺, and CD62L⁺ cells. FSc indicates forward scatter; and SSc, side scatter. (C) Representative flow plots of the intermediate CD4/14/45RA⁻ fraction showing removal (> 98%) of the depleted subsets. (D) Representative flow plots of the CD62L⁻ and CD62L⁺ fractions after the CD62L selection step. The left 2 panels show the phenotype of the CD62L⁻ fraction and the right 3 panels show the phenotype of the CD62L⁺ fraction. Analysis of the CD8⁺CD62L⁺ cells (far right panel) revealed that the most of these cells were CD13⁺ consistent with the selection of a CD62L⁺ myeloid subset that was not removed with the CD4/CD14/CD45RA depletion. (E) Phenotype of the CD8⁺CD62L⁺ fraction for markers of T_{CM}. Data are representative of 5 independent experiments. (F) Summary of enrichment data from independent experiments using PBMCs from 5 different donors showing the total frequency of CD8⁺ T cells and the frequency of CD8⁺ cells that are CD62L⁺. The horizontal line indicates the mean \pm SEM.

For analyses of cytokine secretion, target and effector cells were plated at an E:T ratio of 1:1, and IFN- γ , TNF- α , and IL-2 were measured by Luminex assay (Invitrogen) in the supernatant after 24 hours of incubation.

CFSE proliferation assay

T cells were labeled with 0.2 μ M CFSE (Invitrogen), washed, and plated with stimulator cells at a ratio of 1:1 in CM without IL-2. After 72- or

Table 1. The absolute number of target cells obtained after each selection and the yield of the target fraction

	PBMCs	CD4/CD14/CD45RA-depleted fraction	CD4/CD14/CD45RA-depleted CD62L ⁺ fraction
Cell number	697 × 10 ⁶ (558-1282 × 10 ⁶)	31.2 × 10 ⁶ (23.4-38.6 × 10 ⁶)	8.8 × 10 ⁶ (7.2-13.8 × 10 ⁶)
% CD45RA ⁻ CD8 ⁺ CD62L ⁺	1.7 (0.4-3.3)	16.3 (9.2-25.7)	42.1 (22.5-55.9)*
Yield of CD45RA ⁻ CD8 ⁺ CD62L ⁺ cells†		45.5% (21.3%-88.4%)	25.2% (15.8%-55.5%)

*The majority of non-CD8⁺ cells were CD13⁺CD62L⁺ myeloid cells.

†The yield of CD45RA⁻CD8⁺CD62L⁺ cells was calculated by multiplying the absolute cell number of each fraction and the proportion that were CD45RA⁻CD8⁺CD62L⁺, and dividing by the absolute number of CD45RA⁻CD8⁺CD62L⁺ cells in PBMCs × 100 (%). The data are the summary of 5 experiments.

96-hour incubation, cells were labeled with anti-CD8 mAb and samples were analyzed by flow cytometry, and division of live CD8⁺ T cells was assessed by CFSE dye dilution.

Results

Enrichment of CD45RO⁺CD8⁺CD62L⁺ T_{CM} from PBMCs with clinical grade reagents

We evaluated a 2-step immunomagnetic selection method using clinical-grade reagents to enrich CD8⁺ T_{CM} from PBMCs obtained from healthy donors. CD8⁺ T_{CM} typically comprise less than 3% of PBMCs in healthy donors, and can be identified by expression of the CD45RO isoform that is acquired during the naive to memory transition, and by the coexpression of CD62L.^{22,29} To enrich the CD8⁺ T_{CM} fraction, we first depleted CD4⁺, CD14⁺, and CD45RA⁺ cells from PBMCs using clinical grade mAb conjugated to paramagnetic beads, and then positively selected CD62L⁺ cells with a biotinylated anti-CD62L mAb and clinical-grade anti-biotin beads (Figure 1A). In 5 independent experiments starting with a median of 697 × 10⁶ PBMCs from different donors (Figure 1B), we obtained a median of 31.2 × 10⁶ cells (range, 23.4-38.6 × 10⁶) after the CD4/14/45RA depletion. The cells remaining after depletion contained only very rare contaminating CD4⁺/14⁺/45RA⁺ cells (Figure 1C), and were predominantly (> 60%) CD8⁺ T cells with a median of 16.3% CD45RA⁻CD8⁺CD62L⁺ T_{CM} (range, 9.2%-25.7%; Table 1). After selection of CD62L⁺ cells from the CD4/14/45RA⁻ fraction, we obtained a median of 8.8 × 10⁶ (range, 7.2-13.8 × 10⁶) cells of which a median of 87.7% (range, 84.4%-93.1%) were CD62L⁺ and 56.0% (range, 29.0%-66.0%) were CD8⁺ cells. The CD8⁻ cells that remained in the CD4/14/45RA⁻CD62L⁺ fraction were primarily CD62L⁺ myeloid cells that expressed CD13 and were not removed by the initial density gradient separation (Figure 1D). The fraction of CD8⁺ T cells that expressed CD62L was 83.0% (range, 69.0%-96.0%), and these cells were predominantly CD28⁺ and CD27⁺, which is characteristic of T_{CM} (Figure 1D-F). Contaminating CD4, CD14, CD45RA, CD16, and CD19 cells were very rare in the CD4/14/45RA⁻CD62L⁺ fraction (Table 2). Thus, this 2-step immunomagnetic selection method using clinical-grade mAb-conjugated beads provided approximately 25-fold enrichment of CD8⁺ T_{CM} with an overall yield of 25.2% (range, 15.8%-55.5%; Table 1).

Enrichment of virus-specific T_E cells from T_{CM}

We next examined culture formats that would induce preferential expansion of virus-specific T cells present in the enriched T_{CM} fraction. The T_{CM} cells were cultured with CMV or EBV peptide-pulsed, γ -irradiated PBMCs in either 24-well (10⁶ responder T cells/well) or 96-well plates (10⁴ responder T cells/well), and the frequency of tetramer-positive cells was determined on day 10. The frequency of tetramer positive T cells in the starting T_{CM} population was typically low (< 0.1%) and as expected, the majority of the tetramer-positive cells were CD62L⁺ (Figure 2A, supplemental Figure 2).

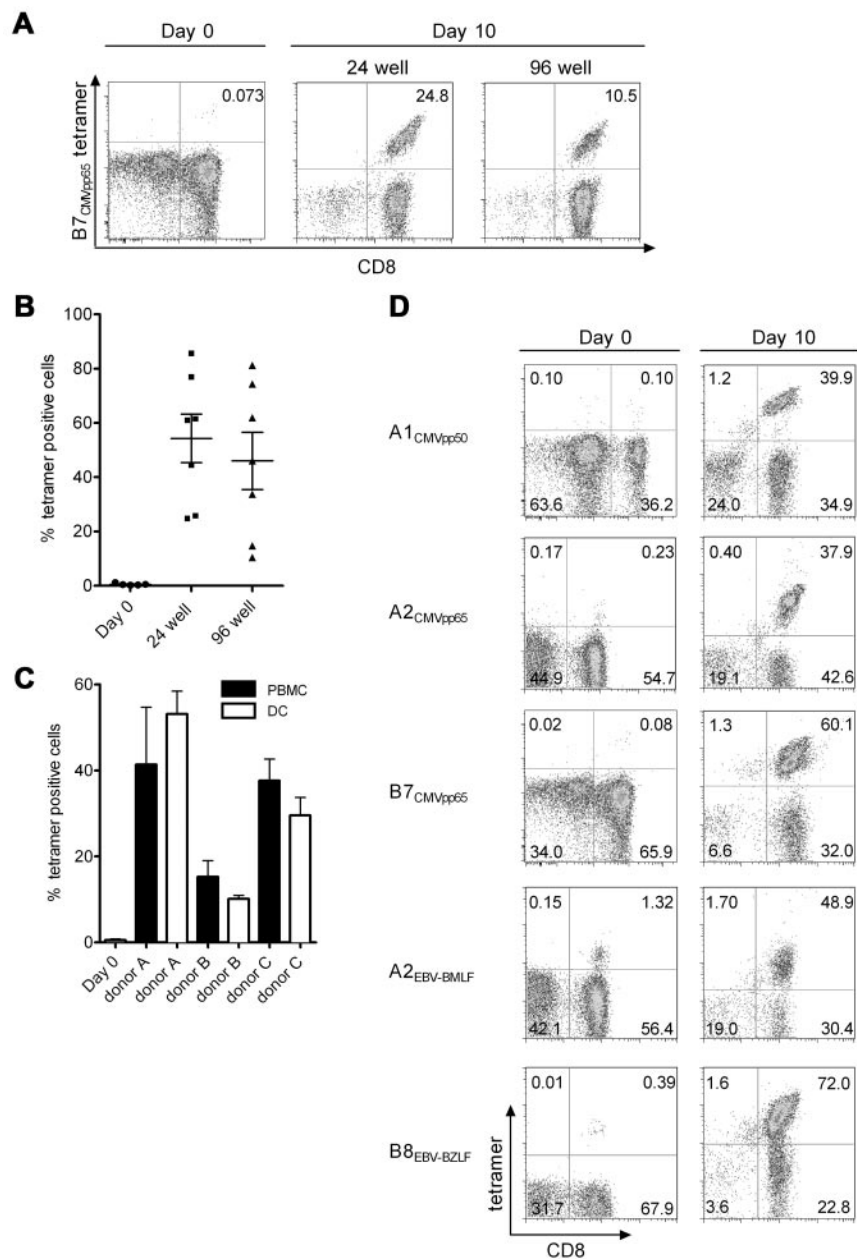
Stimulation with CMV peptides presented by HLA-A*0201 and HLA-B*0702 resulted in a dramatic increase in the tetramer-positive T cells after 10 days both in the 96-well and 24-well culture formats (Figure 2A-B). Of note, the contaminating non-CD8⁺ cells that were present in the starting population declined after 10 days of culture, suggesting these cells do not persist or proliferate under these in vitro culture conditions (Figure 2A,D).

We then evaluated whether γ -irradiated, monocyte-derived DCs might be superior APCs compared with peptide-pulsed PBMCs for inducing expansion of virus-specific T_{CM} in the cultures. There was no significant difference in the frequency of tetramer-positive T cells after 10 days in cultures stimulated with peptide-pulsed PBMCs or DCs (Figure 2C). Thus, for simplicity we used PBMCs as APCs for subsequent experiments to determine whether this method would be generally effective for rapidly enriching T cells specific for multiple epitopes of EBV and CMV presented by other common HLA alleles. In all cases, we observed significant outgrowth of tetramer-positive CD8⁺ T cells, with the 24-well cultures for each of the epitopes containing > 35% tetramer-positive cells after 10 days of expansion (Figure 2D).

Lentiviral transduction of virus-specific T_{CM} and expansion of bi-specific T_E cells

The selective outgrowth of virus-specific T_{CM} after Ag stimulation suggested it might be possible to simultaneously transduce the cells with a CD19-CAR lentivirus during their proliferation to rapidly derive bi-specific T cells. Therefore, we stimulated CD8⁺ T_{CM} with peptide-pulsed PBMCs and added lentivirus supernatant on day 1 followed by spinfection (Figure 3A). After 8-10 days, the cells were examined for tetramer staining to determine the frequency of virus-specific T cells, and for expression of the CAR and tEGFR to determine the frequency of transduced T cells. In 6 independent experiments, the fraction of cells that were tetramer positive was a median of 30.1% (range, 5.8%-94.7%), and the fraction that expressed the CD19-CAR was a median of 21.5% (range, 11.7%-27.9%). A median of 54.9% (range, 15.7%-96.1%) of the tetramer-positive T cells was also CD19-CAR⁺ as assessed by staining for either the Fc portion of the CAR or tEGFR, which is encoded downstream of a T2A sequence in the CAR vector and coordinately expressed with the CAR (Figure 3B). The majority of cultures had only a very minor population of Fc or tEGFR⁺, tetramer-negative cells (Figure 3B). The selective transduction and expansion of virus-specific T cells was observed after stimulations with multiple CMV epitopes (HLA-A*0101_{CMVpp50}; HLA-A*0201_{CMVpp65}; HLA-B*0702_{CMVpp65}) and with EBV epitopes (HLA-A*0201_{EBV-BMLF1}; HLA-B*0801_{EBV-BZLF1}). Thus, simultaneous Ag stimulation and lentiviral transduction was successful in reproducibly deriving a population of T cells that expressed both a virus-specific TCR and a CD19-CAR.

We next evaluated whether subsequent stimulation of the cultures with CD19⁺ APCs would expand the CD19-CAR⁺ T cells and retain the dominant virus-specific fraction. We evaluated an



EBV-transformed LCL line (TM-LCL) that is CD19⁺, HLA-A2 and -B7 negative, and used widely to provide feeder cells for expanding human T cells for clinical adoptive therapy.^{30,31} We tested a range of responder-stimulator ratios and found that a T cell:LCL ratio of 1:7 gave the greatest expansion of CD19-CAR⁺ T cells (Figure 3C), with a total cell yield of > 10¹⁰ T cells more than 2 cycles of stimulation starting from 10⁶ cells. The percentage

of tetramer-positive T cells in the cultures increased similar to CAR-transduced cells despite the absence of stimulation through the virus-specific TCR, although there was variability from culture to culture (Figure 3D right panel).

Purification of bi-specific T_E cells using class I MHC streptamers

T cells specific for CMV and EBV, either selected by in vitro culture or with class I MHC streptamers, have been adoptively transferred to allo-HSCT recipients without causing GVHD.^{17,18,32} Thus, if donor-derived CD19 CAR-modified T cells were to be administered for adoptive immunotherapy to prevent or treat relapse of CD19⁺ malignancies in the allo-HSCT setting, it would be desirable to infuse T-cell products that were predominantly virus specific. Thus, we used reversible class I MHC streptamers to further purify virus-specific T cells from the

Figure 2. Comparison of culture conditions for expanding virus-specific T cells from CD45RA⁻CD62L⁺CD8⁺ precursors. (A) Representative flow plots showing tetramer staining of the enriched CD8⁺CD62L⁺ T_{CM} before and 10 days after stimulation with a B*0702_{CMVpp65} peptide. T_{CM} cells were plated either in a 24-well or 96-well plate with B*0702_{CMVpp65} peptide-pulsed γ -irradiated PBMCs. Shown are data from individual wells of the 24-well cultures and pooled wells of the 96-well cultures. (B) T_{CM} cells from 7 donors were cultured the same as in panel A and tested for tetramer positivity on day 10. T_{CM} from 3 donors were stimulated with an A*0201_{CMVpp65} peptide, and T_{CM} from the other 4 donors were stimulated with a B*0702_{CMVpp65} peptide. Symbols represent the frequency of tetramer-positive T cells in cultures from each individual donor and the horizontal lines indicate the mean \pm SEM. (C) T_{CM} cells were plated onto 96-well plates and stimulated with either peptide-pulsed PBMC (■) or peptide-pulsed DCs (□). After 10 days of culture, 6 to 12 wells with growth were randomly selected and analyzed for the frequency of virus-specific T cells by tetramer staining. For each of the 3 donors, a B*0702_{CMVpp65} peptide was used for stimulation. The graph shows the mean frequency of tetramer positive cells in each donor and SEM at day 10 after each stimulation condition. (D) T_{CM} cells from 4 donors were plated with autologous PBMCs pulsed with CMV or EBV peptides known to be presented by HLA alleles of the donor. The frequency of virus-specific T cells was determined by tetramer staining in the starting population and 10 days after stimulation. Data are representative of 5 independent experiments from each donor.

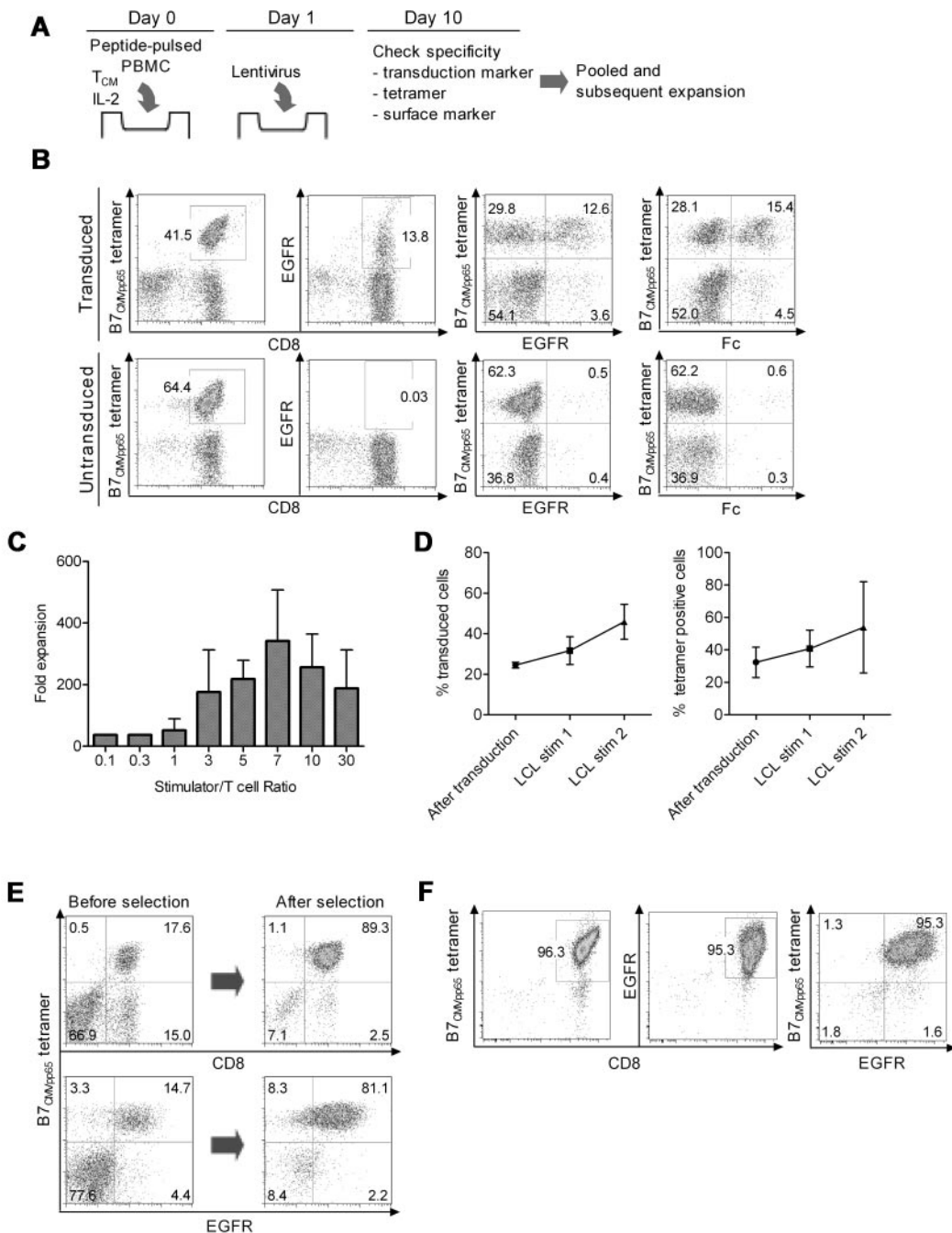


Figure 3. Lentiviral transduction, expansion, and selection of bi-specific T cells. (A) Scheme for simultaneous virus-specific stimulation and CD19-CAR transduction. T_{CM} cells were plated at 10⁶ cells/well into 24-well plates with 10⁶ peptide-pulsed γ -irradiated PBMCs/well and IL-2 (50 IU/mL), and transduced on day 1 with CD19-CAR lentivirus supernatant. (B) Staining of transduced and untransduced T cells with HLA tetramer, anti-Fc, and anti-EGFR reagents after 10 days of culture. Data are shown for a culture stimulated with an HLA-B*0702_{CMVpp65} peptide-pulsed PBMCs. Similar data were obtained for T_{CM} cells stimulated with A*0101_{CMVpp65}, A*0201_{CMVpp65}, A*0201_{EBV-BMLF1}, and B*0801_{EBV-BZLF1} peptides. (C) Growth of bi-specific T cells after stimulation with CD19⁺ EBV-transformed B cells (TM-LCL) at various T-cell:LCL ratios during a 10-day stimulation cycle. Data are pooled from 5 independent experiments and the mean fold expansion in cell number and SEM are shown. (D) CD19-CAR⁺ and tetramer-positive T cells are enriched over 2 cycles of stimulation with CD19⁺ TM-LCL. The bi-specific T cells were stimulated with a 1:7 ratio of TM-LCL, fed with 50 IU/mL IL-2 and the frequency of cells that bound the HLA tetramer and expressed cell-surface EGFR was determined on day 10-13 (left panel, CAR⁺ cells; right panel, tetramer-positive cells). Data are pooled from 5 independent experiments (mean and SEM) with 4 viral epitopes (A*0101_{CMVpp65}, A*0201_{CMVpp65}, B*0702_{CMVpp65}, and A*0201_{EBV-BMLF1}). (E) Purification of tetramer positive bi-specific cells with reversible class I MHC streptamer. Streptamer selection was performed after the first stimulation with CD19⁺ TM-LCLs. Shown are the data for selection of HLA B*0702_{CMVpp65} bi-specific T cells, which is representative of 4 independent experiments with A*0101_{CMVpp65}, A*0201_{CMVpp65}, B*0702_{CMVpp65}, and A*0201_{EBV-BMLF1} streptamers. The yield was a median of 26.9% (range, 15.0%-43.8%). (F) Purity of final bi-specific T_{CM}-derived cell product. After MHC streptamer selection, a second stimulation with TM-LCL was performed and the bi-specific T cells were stained with the class I HLA tetramer and with anti-EGFR on day 10 after stimulation. Data are shown for a bi-specific (B*0702_{CMVpp65}; CD19CAR) T-cell product and are representative of 4 independent experiments.

transduced T-cell cultures after the first stimulation with CD19⁺ LCL.²⁷ Streptamer selection resulted in the reproducible enrichment of virus-specific T cells to > 80% purity (range, 86.0%-

96.8%), of which ~ 85% (range, 80.0%-99.7%) expressed the CD19-CAR. The overall cell yield with streptamer selection was a median of 26.9% (range, 15.0%-43.8%). Importantly, the

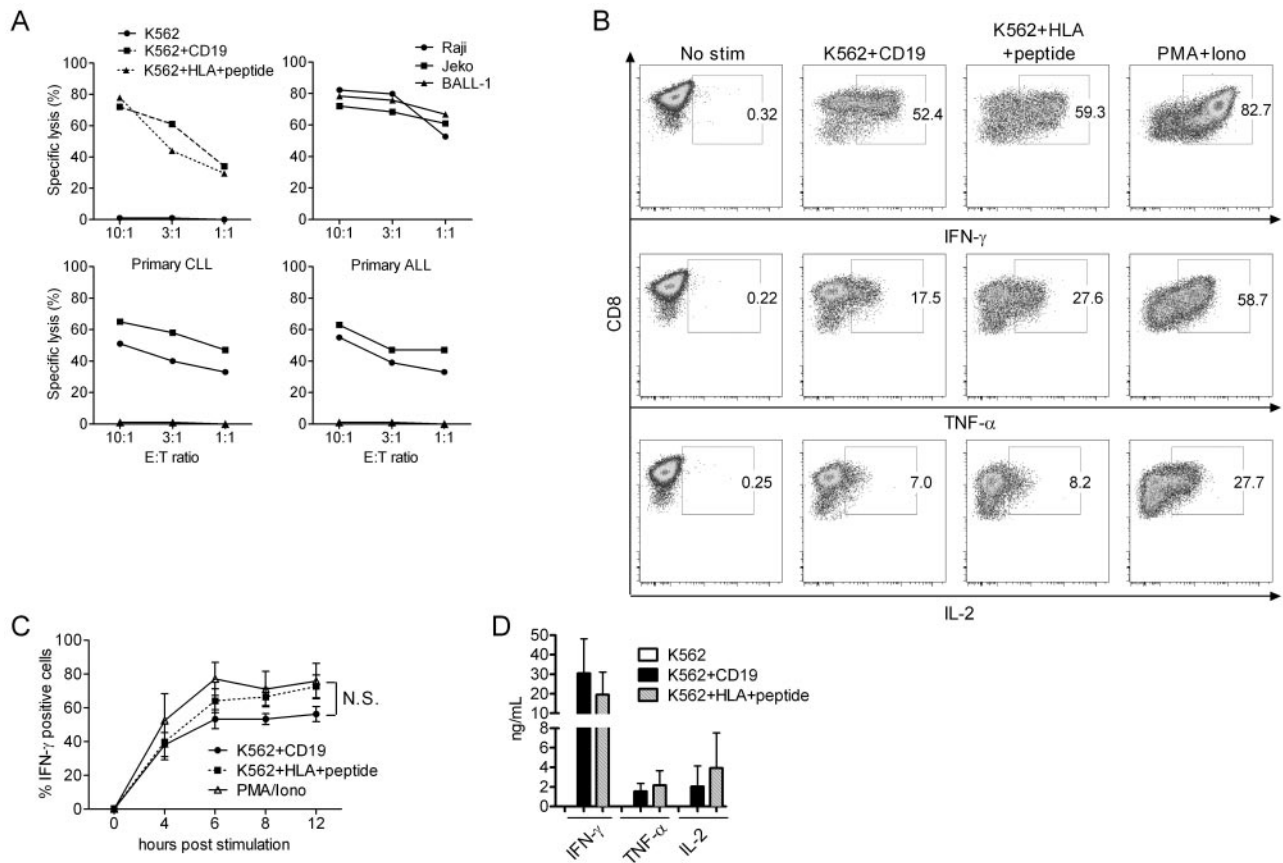


Figure 4. Analysis of effector functions after stimulation of bi-specific T cells through the virus-specific TCRs and CD19-CARs. (A) Cytotoxicity. HLA-B*0702_{CMVpp65} bi-specific T cells were tested for lysis of K562 (●), K562 transduced with CD19 (■), and K562 transduced with HLA-B*0702 and pulsed with CMVpp65 peptide (▲; top left panel). Bi-specific T cells lysed CD19⁺ tumor cell lines (top right panel), primary CLL cells from 2 patients (bottom left panel) and primary ALL cells from 2 patients (bottom right panel). In assays against primary tumor cells, K562 cells were used as a negative control (triangles in the bottom panels). (B) Intracellular cytokine staining. HLA-B*0702_{CMVpp65} bi-specific T cells stimulated for 4 hours with an equal number of the indicated K562 transfectants, permeabilized, and stained for intracellular IFN- γ , TNF- α , and IL-2, or left unstimulated. Stimulation with PMA/ionomycin served as a positive control. Data are shown for B*0702_{CMVpp65} bi-specific T cells and are representative of 5 experiments with bi-specific T cells from different donors. (C) Time-course analyses of intracellular IFN- γ staining of the bi-specific T cells. T cells were stimulated either with the indicated K562 transfectants or with PMA/ionomycin for 4–12 hours, permeabilized, and stained for intracellular IFN- γ . The mean and SEM of the percentage of T cells that stained positive for IFN- γ is shown for 5 independent experiments with bi-specific T cells from 3 donors (N.S., not significant). (D) IFN- γ , TNF- α , and IL-2 secretion. T cells were stimulated with the indicated K562 transfectants at a 1:1 ratio, and culture supernatants were harvested at 24 hours and analyzed by Luminex assay. Data are pooled from 7 independent experiments with bi-specific T cells from 7 donors (mean and SD).

frequency of CD19-CAR-transduced T cells in the selected population that did not stain with the tetramer was < 3% (Figure 3E).

After the streptamer selection, a second stimulation with CD19⁺ LCL was performed to determine whether the high frequency of bi-specific T cells was maintained through an additional expansion cycle. The T cells proliferated equivalently well as those that had not undergone streptamer selection and at the end of the stimulation cycle, the frequency of tetramer-positive and CD19-CAR⁺ cells in the culture increased to ~90% (range, 80.7%-96.3%) and ~85% (range, 77.9%-95.3%), respectively (Figure 3F). Thus, large numbers of highly pure bi-specific T_E cells that are derived from CD8⁺ T_{CM} precursors and engineered to express a CD19-specific chimeric receptor could be readily generated for adoptive immunotherapy of allo-HSCT recipients in ~30–35 days starting from 400 mL of donor peripheral blood.

Analysis of effector functions, signaling, and cell division after stimulation through the virus-specific TCR and CD19-CAR

Prior studies have demonstrated that polyclonal T cells transduced to express a CAR can lyse target cells and secrete cytokines after

stimulation through the CAR, and that incorporation of costimulatory domains such as CD28, 4-1BB, and OX40 into the CAR increases IL-2 production and improves the persistence of the cells in immunodeficient mice.^{14,33} However, CAR binding to its ligand is expected to be structurally distinct from that of a TCR, and a direct comparison of effector functions and signaling through an introduced CAR and the endogenous TCR on the same cell has not been evaluated. To perform this analysis, we transduced K562 tumor cells with the costimulatory molecules CD80 and CD86, and with CD19 or HLA molecules (HLA-A*0201; HLA-B*0702) and sorted cells that expressed each of the transgenes to high purity (> 95%; supplemental Figure 1). The bi-specific T cells that we generated in our cultures efficiently lysed both K562/CD19 and K562/HLA viral peptide-pulsed target cells, in addition to CD19⁺ tumor cell lines, primary CD19⁺ chronic lymphocytic leukemia (CLL) and ALL cells, indicating that lytic function was mediated through both the CAR and the TCR (Figure 4A). IFN- γ , TNF- α , and IL-2 production after ligation of the CD19-CAR or the TCR was evaluated by stimulating aliquots of the bi-specific T cells with each of the K562 transfectants. K562/B*0702_{CMVpp65} stimulation induced a slightly higher percentage of bi-specific T cells to

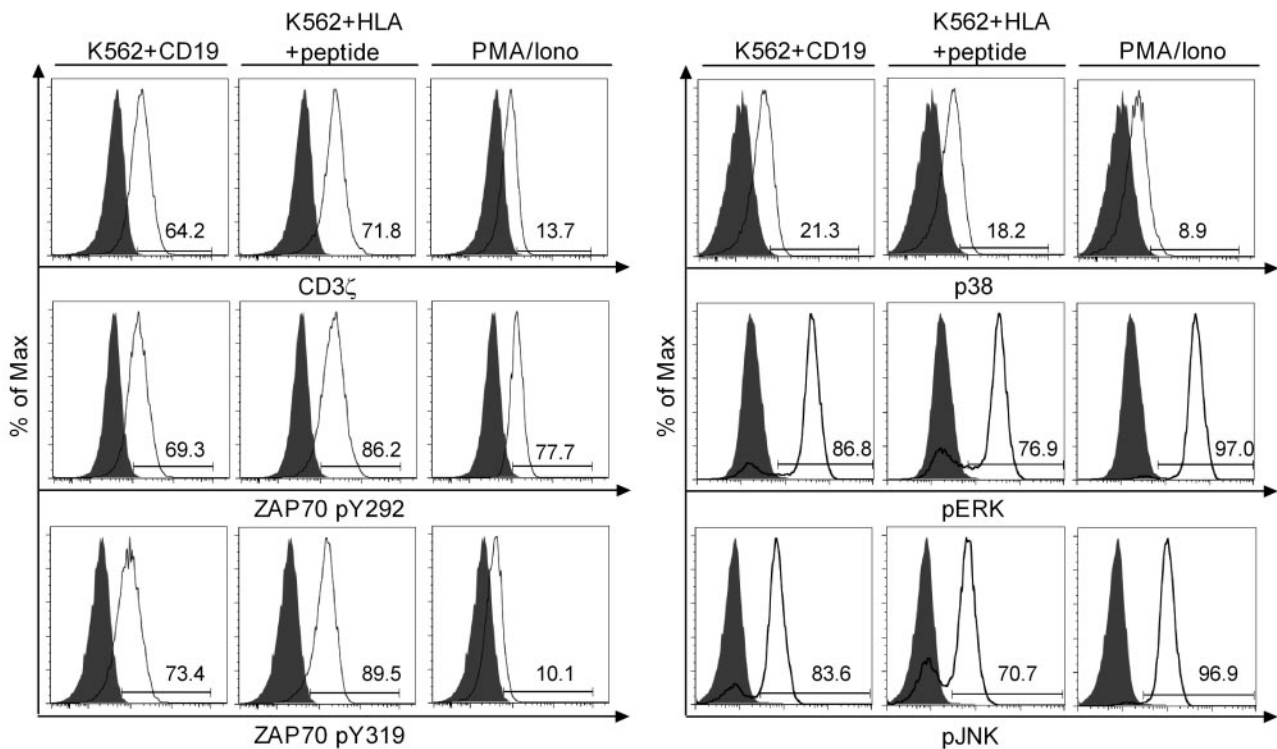


Figure 5. Analysis of intracellular signaling after stimulation through the virus-specific TCRs and CD19-CARs. Intracellular phospho-specific staining of CD3 ζ , ZAP70 (pY292 and pY319), p38, ERK, and JNK. Bi-specific T cells were either stimulated with K562 (gray), the indicated K562 transfectants at a 1:5 ratio, or PMA/ionomycin for 2 minutes (CD3 ζ and ZAP70), or 10 minutes (p38, ERK, and JNK), permeabilized and stained with phospho-specific mAbs, and analyzed by flow cytometry. The flow plots for CD3 ζ , ZAP70, and p38 were performed on a FACSCanto II (BD Biosciences), and for ERK and JNK on a FACSCalibur (BD Biosciences). Data are representative of B*0702_{CMVpp65} bi-specific T cells and representative of 4 independent experiments with bi-specific T cells from 4 donors.

produce IFN- γ , TNF- α and IL-2 by intracellular cytokine staining than K562/CD19 stimulation, but this difference was not statistically significant (Figure 4B-C). We analyzed the rate at which bi-specific T cells became IFN- γ ⁺ by stimulating the cells with each APC for various times before fixation and intracellular staining. In the time-course analysis, \sim 10% more cells secreted IFN- γ after TCR stimulation at time points after 4 hours (Figure 4C). However, IFN- γ , TNF- α , and IL-2 secretion into the culture supernatant was equivalent after CD19 and viral Ag stimulation (Figure 4D). Taken together, these data demonstrate only slight differences in induction of effector functions whether the T cell is signaled through the endogenous TCR or the introduced CAR.

We next examined phosphorylation of proximal and distal signaling molecules including CD3 ζ , ZAP70, p38, ERK, and JNK after Ag binding using flow-based intracellular staining with phospho-specific mAb. A short 2- to 10-minute stimulation with CD19⁺ K562 or K562/B*0702 pulsed with an optimal concentration of B*0702_{CMVpp65} peptide induced phosphorylation of CD3 ζ and ZAP70 at tyrosine 292 and 319 in the majority of T cells. In some but not all experiments, the mean fluorescence intensity of phosphoprotein staining was lower after stimulation through the CAR than through the TCR. However, both the proportion of T cells that exhibited phosphorylation of distal signaling molecules including ERK, JNK, and p38, and the mean fluorescence intensity of staining were not significantly different after stimulation through the CAR or the TCR (Figure 5).

The release of cytolytic granules and cytokines after ligand engagement and signaling through a CAR does not ensure that the CAR-modified T cell will undergo productive cell division after recognition of target cells. We observed similar up-regulation of CD25 on bi-specific T cells after stimulation

through the TCR or the CAR, suggesting the cells would be similarly responsive to endogenous or exogenous IL-2 (Figure 6A). Indeed, CFSE labeling of T cells before stimulation with K562/CD19 or K562/viral Ag in cultures that were not supplemented with IL-2 showed that a comparable proportion of the bi-specific T_{CM}-derived T_E cells divided over 72 and 96 hours (Figure 6B and data not shown). Cell division was more robust after stimulation through the TCR or the CAR than after stimulation with CD3/28 beads (Figure 6B). T-cell proliferation induced by stimulation through either the CD19-CAR or the TCR also resulted in an equivalent increase in absolute cell number in the cultures over 4 days, even in the absence of supplemental IL-2, indicating that ligand engagement through the CAR did not induce greater activation-induced cell death than through the TCR, and that sufficient endogenous IL-2 was produced by T_{CM}-derived T_E cells to promote cell proliferation (Figure 6C). Thus, stimulation of T_{CM}-derived T_E cells through an introduced CD19-CAR that contains a CD28 costimulatory domain induces similar phosphorylation of signaling molecules, production of effector cytokines, and T-cell division as stimulation through an endogenous virus-specific T cell receptor on the same cell.

Discussion

Gene transfer to redirect the specificity of any human T lymphocyte to recognize cancer cells through the expression of a TCR specific for a tumor-associated Ag or a CAR specific for a tumor cell-surface molecule, is a developing area in cancer therapy. Several issues remain to be resolved including the type of T cell

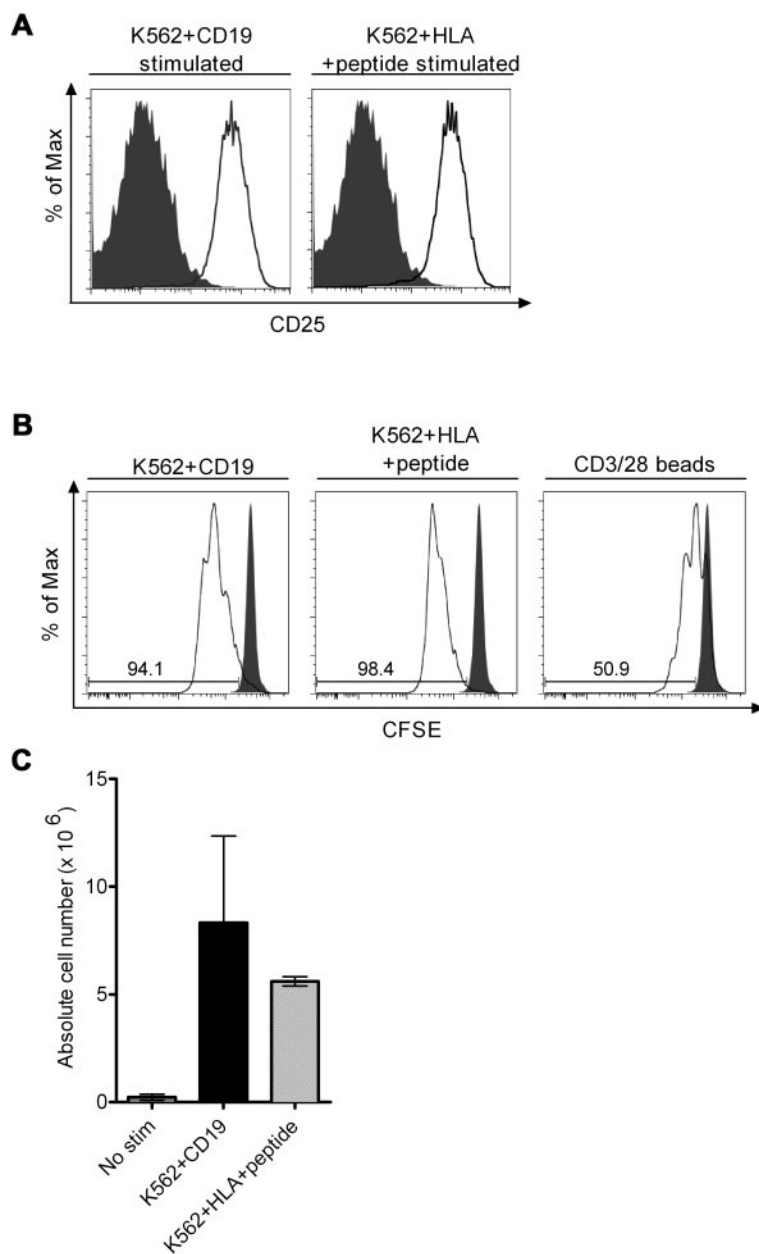


Figure 6. T-cell activation and division after stimulation through the virus-specific TCRs and CD19-CARs. (A) Up-regulation of CD25 after CD19 or TCR stimulation. Bi-specific T cells were stimulated with an equal number of either K562/CD19 or K562/HLA-B*0702 cells pulsed with CMVpp65 peptide or left unstimulated and examined for CD25 expression 24 hours later. Expression of CD25 on unstimulated cells is shown in the gray histograms and expression of CD25 on stimulated T cells is shown in the white histograms. (B) CFSE dilution assay after CD19 or TCR stimulation. Bi-specific T cells were labeled with CFSE, stimulated with an equal number of the indicated K562 transfectants or with CD3/28 beads, and CFSE staining intensity was analyzed 72 hours after stimulation. CFSE staining of unstimulated T cells is shown in the gray histograms and those of stimulated in the white histograms. Data are representative of 3 independent experiments. (C) Cell growth of bi-specific T cells after CD19 or TCR stimulation without exogenous IL-2. A total of 2×10^6 bi-specific T cells were stimulated with either K562/CD19 transfectants or K562/HLA transfectants pulsed with CMV peptide, and the absolute cell count was determined by the standard trypan blue dye exclusion method 4 days after stimulation. Data are pooled from 4 independent experiments with bi-specific T cells from 4 donors. The mean and SD of the absolute cell number is shown.

(naive, central memory, or effector memory) to modify, and the design of receptor constructs that mimic physiologic signals in the engineered T cells. A potential use of gene-modified donor T cells is to induce a GVL effect after allo-HSCT to reduce the unacceptably high rates of relapse that are currently experienced by patients with advanced malignancies.^{1-5,8} The use of T cells from a normal donor circumvents the potential difficulty deriving autologous T-cell products from lymphopenic patients who have had extensive prior chemotherapy, but the application of T-cell therapy after allo-HSCT requires knowledge of the specificity of the endogenous TCR(s) to avoid causing GVHD. Unselected autologous CAR-modified T-cell therapy has recently been reported to exhibit profound antitumor activity in CLL.^{34,35} The methodology described here would enable the application of this approach to more aggressive B-cell malignancies where allo-HSCT is the standard of care and where engineering and infusing unselected donor T cells would carry a risk of GVHD. We show that bi-specific (CD19-CAR, virus-specific) CD8⁺ T_E cells can be rapidly derived from

T_{CM} precursors of normal donors. We selected T_{CM} cells for genetic modification because they exhibit superior proliferation to Ag compared with T_{EM} cells,²² and we have shown that gene-modified virus-specific T_E cells derived from T_{CM} cells, but not from T_{EM} cells, persist long-term after adoptive transfer in animal models.^{21,23} To select CD8⁺ T_{CM}, we used 3 mAbs (CD4, CD45RA, and CD14) for depletion of undesired cells and a CD62L mAb for positive enrichment. This 2-step depletion and enrichment was highly effective in removing and selecting the desired subsets, and enriched for CD8⁺CD62L⁺ memory cells, although a CD62L⁺ CD13⁺ myeloid population that phenotypically and morphologically resembled basophils remained after enrichment. The proportion of contaminating CD13⁺ cells varied between donors; however, these cells did not persist in culture and did not significantly alter T-cell proliferation or transduction efficiency.

We focused on deriving CMV- and EBV-specific T cells from T_{CM} for genetic modification because a majority of donors retain virus-specific CD8⁺ memory T cells for these pathogens, and the adoptive transfer of virus-specific T cells for even a few epitopes

after allo-HSCT confers antiviral immunity to immunodeficient HSCT recipients without causing GVHD.^{17-19,36} It has been suggested that CAR-modified virus-specific T_E cells may exhibit superior persistence in vivo as a consequence of signals delivered through the virus-specific TCR.^{37,38} The frequency and proportion of the memory CD8⁺ T-cell response to CMV and EBV that resides in the CD62L⁺ T_{CM} subset varied for each virus and among individuals, but we could reliably derive T_E cells for multiple HLA class I-restricted epitopes from both viruses from a majority of donors. In addition, the addition of lentivirus shortly after Ag stimulation led to efficient and preferential transduction of the virus-specific T cells, which could then be expanded in short-term culture by stimulation through the CAR. We show that selection with reversible MHC streptamers as a final enrichment provides highly pure populations of bi-specific T cells, and avoids transferring T cells that could cause GVHD. It is possible that an additional benefit of this therapy is that the virus-specific CTL would provide antiviral protection in the post-allo-HSCT setting, although the consequences of inserting a CAR on TCR signaling in vivo are uncertain, and will require careful analysis in the clinical application of this approach.

The derivation of highly pure human T_E cells that expressed both a virus-specific TCR and a tumor-targeting CAR enabled comparative analysis of signaling through the naturally expressed TCR and the introduced CAR on the same T cells. For these studies, we used K562 cells that could present CD19 to the CAR or HLA/peptide complexes to the TCR as APC to control for potential differences in adhesion or other molecules that might be differentially expressed if tumor cells and virus-infected cells were used as APCs. We found that ligation of the TCR and CAR evoked uniform phosphorylation of CD3 ζ , ZAP70, ERK, JNK, and p38 and induced similar secretion of IFN- γ , TNF- α , and IL-2. Moreover, signaling through either the TCR or the CAR resulted in target cell lysis, and induced proliferation and expansion of the T cells in the absence of exogenous IL-2. The CD19-specific CAR used in our study has a CD28 signaling domain in tandem with CD3 ζ , based on prior work showing that addition of CD28 improves proliferation and IL-2 and IFN- γ secretion.¹⁴ The incorporation of additional signaling domains from CD134 or CD137 has been shown to further increase cytokine secretion and lytic activity, and to improve cell viability in vitro and in a xenogeneic mouse engraftment model.³⁹⁻⁴² It is likely that the cellular response to signaling through a CAR will depend on many factors including the specificity and affinity of the scFv component of the CAR, incorporation of costimulatory signaling domains, and ligand density and location on the target cell. The strategy of deriving

highly pure bi-specific T cells allows comparative analysis of signaling events induced by ligation of different CAR constructs with those after endogenous TCR signaling, and may prove useful in selecting the features for individual CARs that more closely approximate physiologic signaling, and preserve T-cell function and survival in vivo.

Our results also have implications for clinical applications of CAR-modified T cells beyond allo-HSCT. The T-cell pool in humans contains a diversity of phenotypic and functionally distinct T cells that have different effector functions and migratory capacity that are imprinted by earlier Ag experience.⁴³ Moreover, the frequency of these subsets of T cells varies substantially from person to person depending on age and pathogen exposure, and may be altered in cancer patients by the type and extent of prior chemotherapy.^{44,45} Thus, transduction of bulk populations of autologous T cells may not provide cell products with uniform capacity to survive, mediate desired antitumor effector function, and migrate in vivo. The strategy of purifying defined subsets of T cells, including those with a defined TCR specificity before genetic modification may provide cell products that have more predictable activity after adoptive transfer.

Acknowledgments

This work was supported by grants from Advanced Clinical Research Organization, Japan Clinical Research Support Unit (S.T.), National Institutes of Health (NIH) CA136551 and CA107399, Nesvig Foundation (M.C.J.), and NIH CA18029, CA114536, and CA136551 (S.R.R.).

Authorship

Contribution: S.T. designed and performed experiments, analyzed the data, and wrote the manuscript; T.N.Y. designed and performed experiments, and analyzed data; R.A.G. performed experiments and analyzed data; C.J.T. performed experiments and helped write the manuscript; M.C.J. contributed reagents and helped write the manuscript; and S.R.R. designed experiments, analyzed the data, and wrote the manuscript.

Conflict-of-interest disclosure: The authors declare no competing financial interests.

Correspondence: Stanley R. Riddell, MD, Program in Immunology, Fred Hutchinson Cancer Research Center, 1100 Fairview Ave North, D3-100, Seattle, WA 98109-1024; e-mail: sriddell@fhcr.org.

References

- Pui CH, Evans WE. Treatment of acute lymphoblastic leukemia. *N Engl J Med*. 2006;354(2):166-178.
- Hunault M, Harousseau JL, Delain M, et al. Better outcome of adult acute lymphoblastic leukemia after early genoidentical allogeneic bone marrow transplantation (BMT) than after late high-dose therapy and autologous BMT: a GOELAMS trial. *Blood*. 2004;104(10):3028-3037.
- Thomas X, Boiron JM, Huguet F, et al. Outcome of treatment in adults with acute lymphoblastic leukemia: analysis of the LALA-94 trial. *J Clin Oncol*. 2004;22(20):4075-4086.
- Bader P, Kreyenberg H, Henze GH, et al. Prognostic value of minimal residual disease quantification before allogeneic stem-cell transplantation in relapsed childhood acute lymphoblastic leukemia: the ALL-REZ BFM Study Group. *J Clin Oncol*. 2009;27(3):377-384.
- Mielcarek M, Storer BE, Flowers ME, Storb R, Sandmaier BM, Martin PJ. Outcomes among patients with recurrent high-risk hematologic malignancies after allogeneic hematopoietic cell transplantation. *Biol Blood Marrow Transplant*. 2007;13(10):1160-1168.
- Collins RH, Goldstein S, Giral S, et al. Donor leukocyte infusions in acute lymphocytic leukemia. *Bone Marrow Transplant*. 2000;26(5):511-516.
- Lutz C, Massenkeil G, Nagy M, et al. A pilot study of prophylactic donor lymphocyte infusions to prevent relapse in adult acute lymphoblastic leukemia after allogeneic hematopoietic stem cell transplantation. *Bone Marrow Transplant*. 2008;41(9):805-812.
- Schmitz N, Dreger P, Glass B, Sureda A. Allogeneic transplantation in lymphoma: current status. *Haematologica*. 2007;92(11):1533-1548.
- Riddell SR. Finding a place for tumor-specific T cells in targeted cancer therapy. *J Exp Med*. 2004;200(12):1533-1537.
- Kolb HJ. Graft-versus-leukemia effects of transplantation and donor lymphocytes. *Blood*. 2008;112(12):4371-4383.
- Dudley ME, Wunderlich JR, Robbins PF, et al. Cancer regression and autoimmunity in patients after clonal repopulation with antitumor lymphocytes. *Science*. 2002;298(5594):850-854.
- Jena B, Dotti G, Cooper LJ. Redirecting T-cell specificity by introducing a tumor-specific chimeric antigen receptor. *Blood*. 2010;116(7):1035-1044.
- Hudecek M, Anderson Jr LD, Nishida T, Riddell SR.

- Adoptive T-cell therapy for B-cell malignancies. *Expert Rev Hematol*. 2009;2(5):517-532.
14. Kowolik CM, Topp MS, Gonzalez S, et al. CD28 costimulation provided through a CD19-specific chimeric antigen receptor enhances *in vivo* persistence and antitumor efficacy of adoptively transferred T cells. *Cancer Res*. 2006;66(22):10995-11004.
 15. Jensen MC, Popplewell L, Cooper LJ, et al. Anti-transgene rejection responses contribute to attenuated persistence of adoptively transferred CD20/CD19-specific chimeric antigen receptor redirected T cells in humans. *Biol Blood Marrow Transplant*. 2010;16(9):1245-1256.
 16. Cooper LJ, Topp MS, Serrano LM, et al. T-cell clones can be rendered specific for CD19: toward the selective augmentation of the graft-versus-B-lineage leukemia effect. *Blood*. 2003;101(4):1637-1644.
 17. Walter EA, Greenberg PD, Gilbert MJ, et al. Reconstitution of cellular immunity against cytomegalovirus in recipients of allogeneic bone marrow by transfer of T-cell clones from the donor. *N Engl J Med*. 1995;333(16):1038-1044.
 18. Leen AM, Christin A, Myers GD, et al. Cytotoxic T lymphocyte therapy with donor T cells prevents and treats adenovirus and Epstein-Barr virus infections after haploidentical and matched unrelated stem cell transplantation. *Blood*. 2009;114(19):4283-4292.
 19. Bollard CM, Kuehnle I, Leen A, Rooney CM, Heslop HE. Adoptive immunotherapy for post-transplantation viral infections. *Biol Blood Marrow Transplant*. 2004;10(3):143-155.
 20. Till BG, Jensen MC, Wang J, et al. Adoptive immunotherapy for indolent non-Hodgkin lymphoma and mantle cell lymphoma using genetically modified autologous CD20-specific T cells. *Blood*. 2008;112(6):2261-2271.
 21. Berger C, Jensen M, Lansdorp P, Gough M, Elliott C, Riddell S. Adoptive transfer of effector CD8⁺ T cells derived from central memory cells establishes persistent T cell memory in primates. *J Clin Invest*. 2008;118(1):294-305.
 22. Lanzavecchia A, Sallusto F. Understanding the generation and function of memory T cell subsets. *Curr Opin Immunol*. 2005;17(3):326-332.
 23. Wang X, Berger C, Wong CW, Forman SJ, Riddell SR, Jensen MC. Engraftment of human central memory-derived effector CD8⁺ T cells in immunodeficient mice. *Blood*. 2011;117(6):1888-1898.
 24. Kumar A, Petri ET, Halmos B, Boggon TJ. Structure and clinical relevance of the epidermal growth factor receptor in human cancer. *J Clin Oncol*. 2008;26(10):1742-1751.
 25. Wang X, Chang WC, Wong CW, et al. A transgene encoded cell surface polypeptide for selection, *in vivo* tracking, and ablation of engineered cells. *Blood*. 2011;118(5):1255-1263.
 26. Dauer M, Schad K, Herten J, et al. FastDC derived from human monocytes within 48 h effectively prime tumor antigen-specific cytotoxic T cells. *J Immunol Methods*. 2005;302(1-2):145-155.
 27. Neudorfer J, Schmidt B, Huster KM, et al. Reversible HLA multimers (Streptamers) for the isolation of human cytotoxic T lymphocytes functionally active against tumor- and virus-derived antigens. *J Immunol Methods*. 2007;320(1-2):119-131.
 28. Riddell SR, Rabin M, Geballe AP, Britt WJ, Greenberg PD. Class I MHC-restricted cytotoxic T lymphocyte recognition of cells infected with human cytomegalovirus does not require endogenous viral gene expression. *J Immunol*. 1991;146(8):2795-2804.
 29. Oberdoerffer S, Moita LF, Neems D, Freitas RP, Hachon N, Rao A. Regulation of CD45 alternative splicing by heterogeneous ribonucleoprotein, hnRNPLL. *Science*. 2008;321(5889):686-691.
 30. Brodie SJ, Lewinsohn DA, Patterson BK, et al. *In vivo* migration and function of transferred HIV-1-specific cytotoxic T cells. *Nat Med*. 1999;5(1):34-41.
 31. Warren EH, Fujii N, Akatsuka Y, et al. Therapy of relapsed leukemia after allogeneic hematopoietic cell transplantation with T cells specific for minor histocompatibility antigens. *Blood*. 2010;115(19):3869-3878.
 32. Schmitt A, Tonn T, Busch DH, et al. Adoptive transfer and selective reconstitution of streptamer-selected cytomegalovirus-specific CD8⁺ T cells leads to virus clearance in patients after allogeneic peripheral blood stem cell transplantation. *Transfusion*. 2011;51(3):591-599.
 33. Kochenderfer JN, Feldman SA, Zhao Y, et al. Construction and preclinical evaluation of an anti-CD19 chimeric antigen receptor. *J Immunother*. 2009;32(7):689-702.
 34. Kalos M, Levine BL, Porter DL, et al. T cells with chimeric antigen receptors have potent antitumor effects and can establish memory in patients with advanced leukemia. *Sci Transl Med*. 2011;3(95):95ra73.
 35. Porter DL, Levine BL, Kalos M, Bagg A, June CH. Chimeric antigen receptor-modified T cells in chronic lymphoid leukemia. *N Engl J Med*. 2011;365(8):725-33.
 36. Wherry EJ, Ahmed R. Memory CD8 T-cell differentiation during viral infection. *J Virol*. 2004;78(11):5535-5545.
 37. Savoldo B, Rooney CM, Di Stasi A, et al. Epstein Barr virus specific cytotoxic T lymphocytes expressing the anti-CD30zeta artificial chimeric T-cell receptor for immunotherapy of Hodgkin disease. *Blood*. 2007;110(7):2620-2630.
 38. Pulè MA, Savoldo B, Myers GD, et al. Virus-specific T cells engineered to coexpress tumor-specific receptors: persistence and antitumor activity in individuals with neuroblastoma. *Nat Med*. 2008;14(11):1264-1270.
 39. Finney HM, Akbar AN, Lawson AD. Activation of resting human primary T cells with chimeric receptors: costimulation from CD28, inducible costimulator, CD134, and CD137 in series with signals from the TCR zeta chain. *J Immunol*. 2004;172(1):104-113.
 40. Pulè MA, Straathof KC, Dotti G, Heslop HE, Rooney CM, Brenner MK. A chimeric T cell antigen receptor that augments cytokine release and supports clonal expansion of primary human T cells. *Mol Ther*. 2005;12(5):933-941.
 41. Zhao Y, Wang QJ, Yang S, et al. A herceptin-based chimeric antigen receptor with modified signaling domains leads to enhanced survival of transduced T lymphocytes and antitumor activity. *J Immunol*. 2009;183(9):5563-5574.
 42. Milone MC, Fish JD, Carpenito C, et al. Chimeric receptors containing CD137 signal transduction domains mediate enhanced survival of T cells and increased antileukemic efficacy *in vivo*. *Mol Ther*. 2009;17(8):1453-1464.
 43. Turtle CJ, Riddell SR. Genetically retargeting CD8⁺ lymphocyte subsets for cancer immunotherapy. *Curr Opin Immunol*. 2011;23(2):299-305.
 44. Mackall CL, Fleisher TA, Brown MR, et al. Distinctions between CD8⁺ and CD4⁺ T-cell regenerative pathways result in prolonged T-cell subset imbalance after intensive chemotherapy. *Blood*. 1997;89(10):3700-3707.
 45. Turtle CJ, Swanson HM, Fujii N, Estey EH, Riddell SR. A distinct subset of self-renewing human memory CD8⁺ T cells survives cytotoxic chemotherapy. *Immunity*. 2009;31(5):834-844.